# Behavioral model and simulator for the Multi-slit Optimized Spectrometer (MOS)


Nicholas Tufillaro[a], Curtiss O. Davis[a], Tim Valle[b], William Good[b], Michelle Stephens[b], and Peter Spuhler[b]

[a]College of Earth, Ocean and Atmospheric Sciences,
Oregon State University, Corvallis, OR 97331
[b]Ball Aerospace, Boulder, CO 80301



## ABSTRACT

The Multi-Slit Optimized Spectrometer (MOS) is a NASA funded Instrument Incubator Program (IIP) to advance an innovative dispersive spectrometer concept in support of the GEO-CAPE ocean science mission. As part of the instruments design and testing, we constructed a 'behavioral model' of the instrument's optical engine which allows an end-to-end simulation from input radiances to final product maps. Here we describe the model used for a rapid, but realistic, simulation of the MOS optical engine, and give illustrative examples of quantitatively tracking errors in the imaging chain from input radiances to bounds on final product errors.



**Keywords:** spectrometer, ocean color, GEO-CAPE, simulator


## 1. INTRODUCTION

End-to-end simulators are playing an increasing role in the construction and use of imaging spectrometers.[1,2] In addition to aiding engineering design and evaluation, simulators can also be a sandbox for testing new signal correction and product algorithms.[3,4] The Multi-Slit Optimized Spectrometer (MOS) is a NASA funded Instrument Incubator Program (IIP) to advance an innovative dispersive spectrometer concept in support of the GEO-CAPE ocean science mission.[5,6] As part of the instruments design and testing, we constructed a 'behavioral model' of the instrument's optical engine which allows an end-to-end simulation from input radiances to final product maps. The MOS SIMulator (MOS-SIM) is a tool designed to enable:

- Producing products at 'first light' for MOS,
- Tracking uncertainties at all stages of imaging and product generation,
- Making informed design trade-offs using information about uncertainties in target products,
- Creating and testing new signal correction and product methods.

A flow diagram showing the steps from the MOS-SIM to final product evaluation, and feedback to enable informed decisions about engineering trade-offs, is shown in Fig. 1.

## 2. DESIGN

The MOS-SIM was constructed before the final assembly of the MOS using data from an optical simulator used to prototype the MOS design. The primary reason for creating the simulator early on in the project was to enable the creation of hyperspectral algorithms to test the design and calibration of MOS before 'first light,' as well as enabling the initial debugging of atmospheric correction and product algorithms before the completion of the optical assembly. MOS-SIM generates 'synthetic data' using three components: the Scene Simulator, the MOS Instrument Simulator, and the Product Generator which includes atmospheric correction (Fig. 2). The backbone of the simulator is a sequence of functions written in MATLAB which call open source or shareware codes where indicated.


Imaging Spectrometry XVIII, edited by Pantazis Mouroulis, Thomas S. Pagano, Proc. of SPIE
Vol. 8870, 88700E · © 2013 SPIE · CCC code: 0277-786X/13/$18 · doi: 10.1117/12.2023526

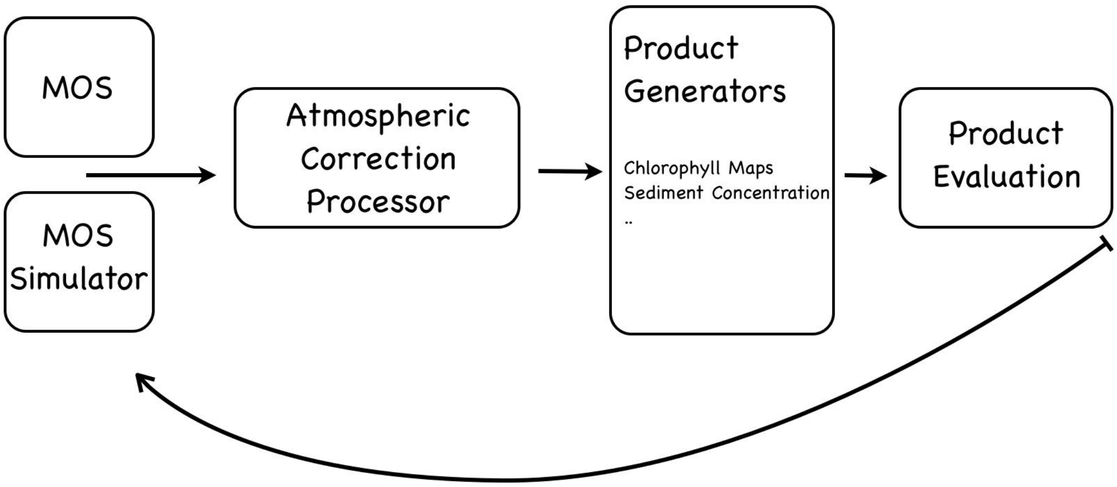


Figure 1. Flow diagram showing steps in going from the MOS Simulator (MOS-SIM) to final product evaluation.

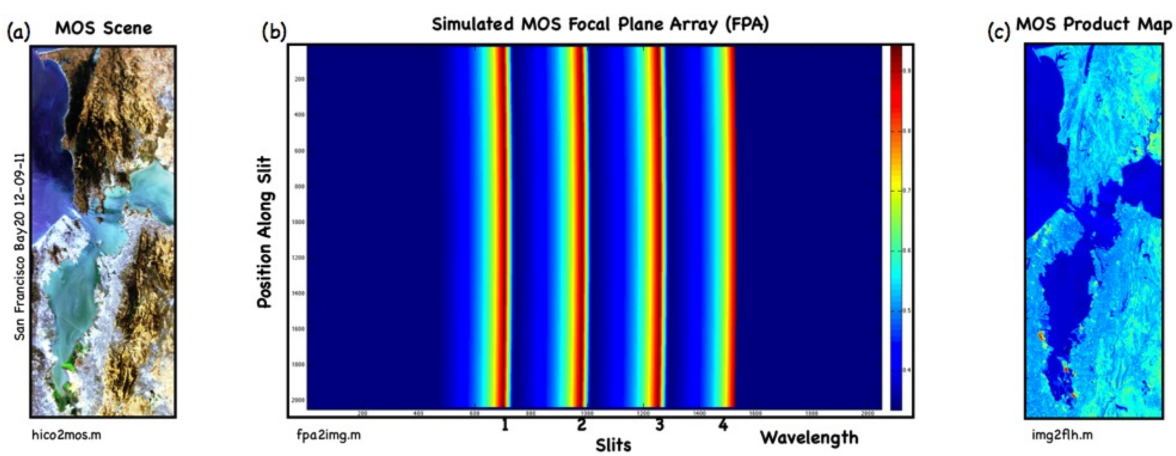


Figure 2. Main components of MOS-SIM. (a) Scene Simulator generates synthetic scenes for input to MOS-SIM based on HICO$^{TM}$ images. (b) Focal plane array generated by simulator. (c) Example product (Fluorescence Line Height Map).

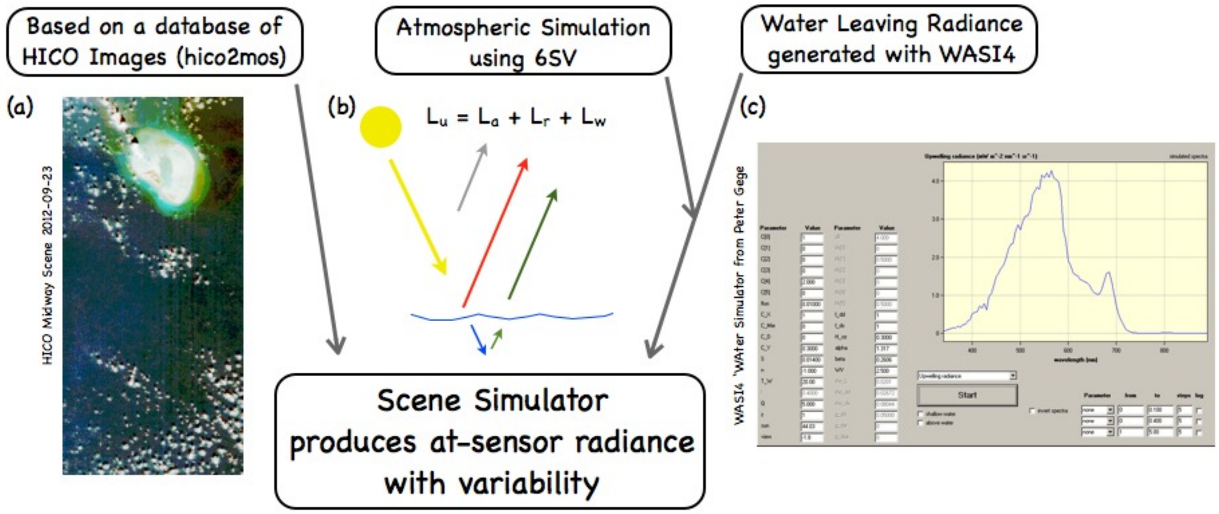


Figure 3. MOS-SIM scene simulator (a) HICO$^{TM}$ provides realistic scene parameters.[7] (b) Top-of-Atmosphere Radiance ($L_u$) is generated from water leaving radiance ($L_w$), surface reflection ($L_r$), and simulated atmospheric scatter ($L_a$). (c) Water leaving radiance simulated using bio-optical models for absorbing and scattering water constituents generated by WASI4.[8]

## 2.1 SYNTHETIC SCENE GENERATION

To generate realistic data we start with hyperspectral images from HICO$^{TM}$.[7] We can input either HICO scenes into the the front end of the simulator, or 'simulations' of HICO scenes which allows us to start with exactly known water and atmospheric parameters. For simulated scenes, we start with a particular HICO scene (e.g. San Francisco Bay, 11 October 2012 in Fig. 2(a)), extract the view and sun angles, simulate typical atmospheric scatter with the code 6SV,[9] and compute the water leaving radiance with predefined optical properties using the code WASI4,[8] which provides a wide variety of specific sediment and algal species models, as well as typical empirical models for CDOM and chlorophyll. The specific choice of model parameters fixes the Inherent Optical Properties (IOP's) for a given pixel. We don't simulated the whole scene, but only an ensemble of typical pixels with a Gaussian variance in the model or IOP parameters. If we use a HICO scene directly for the input, then a Gaussian ensemble of Top-of-Atmosphere (TOA) radiances starting with the HICO image pixels is generated.

In either case, the input to MOS-SIM is typically an 'ensemble' of images where the pixels have a predefined Gaussian variation. Plotting this variation as a histogram provides an approximation to the Probability Distribution Function (PDF), and we track the mean and variance of the PDF at different points of the image chain to gauge the 'uncertainty' of a specific a specific image, operation, or product. Strictly speaking, the transformations along the image chain are nonlinear, thus the PDF is not Gaussian at later stages of the image chain. However, the simplicity of the description of uncertainty by mean and variance alone appears sufficient in this application.

## 2.2 OPTICAL SIMULATION

Since the uncertainties are tracked using a Monte Carlo method, the optical simulation needs to be very fast. We achieve speed through extensive use of look up tables. Specifically, regions on the frontal assembly of MOS are assigned a coordinate which gets uniquely mapped by a ray as it passes through the optical assembly to one of the 2048 x 2048 pixels on the Focal Plane Array (FPA). Furthermore, each pixel on the FPA is assigned a precomputed Point Spread Function (PSF) as determined by the engineering design simulation. Additional look up tables are created for the spectral dispersion of the prism and the model for the read-out electronics. The only real computation beyond look up tables is the convolution operation for the PSF along the FPA (Fig. 4).

To show how the look up tables are indexed, consider the 'Forward Map' for ray optics step in the simulation where the notation is specified in Fig. 5. The forward map notation is written as:

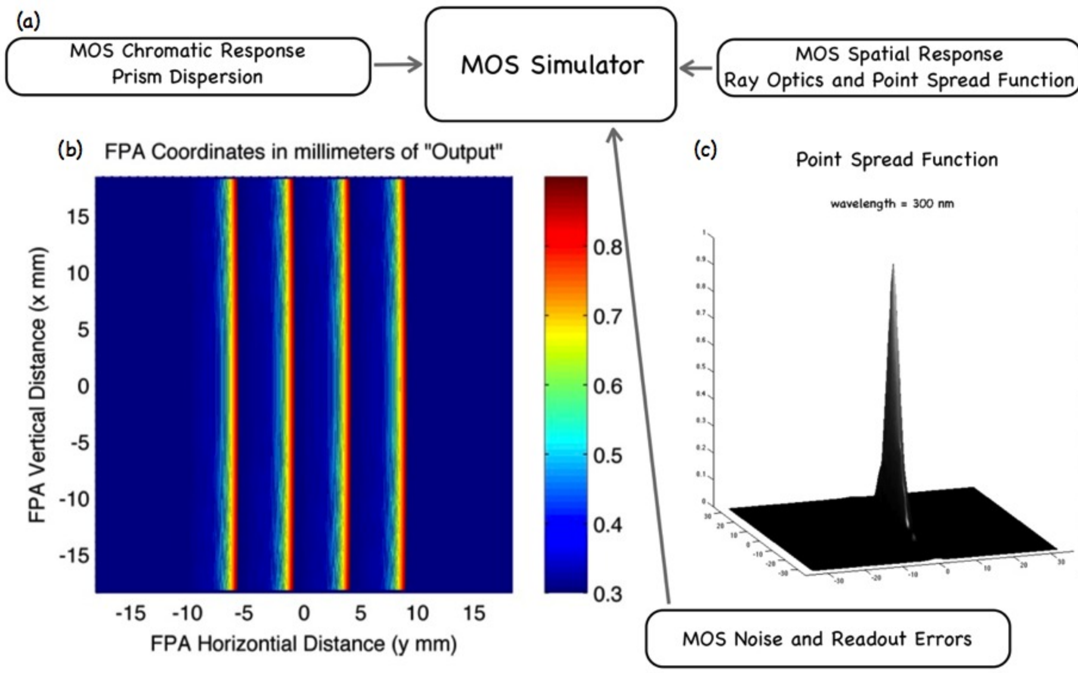


Figure 4. MOS-SIM Optical Simulation (a) Block diagram of sub-modules. (b) Focal Plane Array (FPA) image. (c) Example of Point Spread Function.

$$I(i,j) = \sum_k J_k \tag{1}$$

$$\bar{j}_i = j_i + m(i,j,k) \tag{2}$$

$$\bar{k}_i = k_i + n(i,j,k) \tag{3}$$

$$\bar{I}_{prod}(i,\bar{j},\bar{k}) = \mathcal{F}(\mathcal{G}((\bar{J}_i(\bar{j},\bar{k}))). \tag{4}$$

$\mathcal{G}$ is the calibration step, and $\mathcal{F}$ is the product algorithm. If there is an implicit functional relationship between the 'independent' variables $(i,j,k)$, this can be used to further reduce the number of independent variables. The original MOS design simulations explicitly gives us a map:

$$(x,y,z,J(z,y,z)) \mapsto (\bar{x},\bar{y},\bar{J}(x,y,z)). \tag{5}$$

And to get the 'forward map',

$$(k,j,J_i(j,k)) \mapsto (\bar{k},\bar{j},\bar{J}_i(j,k)) \tag{6}$$

the data is 'binned' into 2048 buckets determined by the pixel size and original engineering simulation.

Models of instrument artifacts, such as optical distortion, noise (optical and electronic) and read out errors (electronic) are added to this forward map model, as well as calibrations to remove the systematic signal distortions. After the MOS assembly, the engineering simulation data that goes into MOS-SIM will be replaced by experimental measurements.

## 2.3 EXAMPLE OF TRACKING UNCERTAINTY

Examples of tracking the mean value and standard deviation of the radiance for Level-1 (L1) calibrated spectra, and Level-2 (L2) atmospheric corrected spectra are shown in Fig. 6.

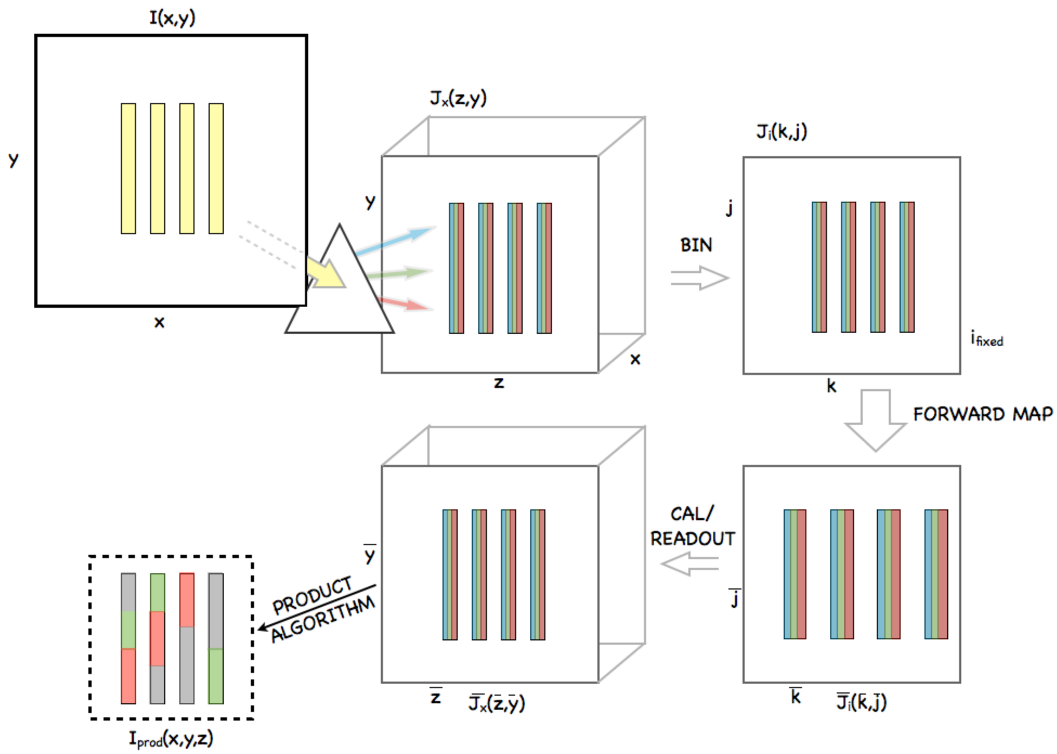


Figure 5. Outline of notation used to index look up tables for the simulation of MOS.

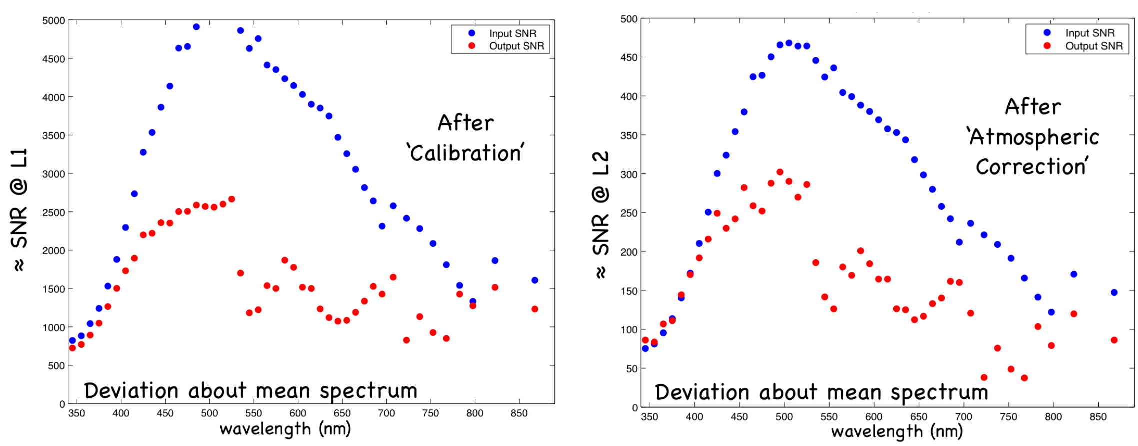


Figure 6. Signal-to-noise ratio (SNR) estimated as $\mu/\sigma$(mean/standard deviation) of input and output radiance at (a) Level-1 and (b) Level-2.

## 3. CONCLUSION

We provided an overview of MOS-SIM. The tool allows us to generate ocean color products, with uncertainties, at the 'first light' of MOS. Using precomputed look up tables allows rapid simulation of an ensemble of images with known ocean and atmospheric parameters, and their variation, and this information can be used to gauge track the uncertainty of ocean products, which is useful both for the final product use, as well as for making informed engineering trade-offs in the design of the imaging spectrometer.

## REFERENCES


[1] Kerekes, J. P., Baum, J. E., and Farrar, K. E., "Analytical model of hyperspectral system performance," in [*Proceedings of Infrared Imaging Systems: Design, Analysis, Modeling and Testing X, SPIE*], 155–166 (1999).

[2] Coppo, P., Chiarantini, L., and Alparone, L., "Design and validation of an end-to-end simulator for imaging spectrometers," *Optical Engineering* **51**(11), 111721–1–111721–14 (2012).

[3] Meola, J., Eismann, M. T., Moses, R. L., and Ash, J. N., "Modeling and estimation of signal-dependent noise in hyperspectral imagery," *Appl. Opt.* **50**, 3829–3846 (Jul 2011).

[4] Uss, M. L., Vozel, B., Lukin, V. V., and Chehdi, K., "Maximum likelihood estimation of spatially correlated signal-dependent noise in hyperspectral images," *Optical Engineering* **51**(11), 111712–1–111712–11 (2012).

[5] Valle, T., Hardesty, C., Davis, C. O., Tufillaro, N., Stephens, M., Good, W., and Spuhler, P., "Multislit optimized spectrometer for ocean color remote sensing," Published in SPIE Proceedings Volume 8510: Earth Observing Systems XVII, 85100C–5 (2012).

[6] Valle, T., Hardesty, C., Davis, C. O., Tufillaro, N., Good, W., Seckar, C., and Spuhler, P., "Multislit optimized spectrometer for ocean color remote sensing: fabrication and assembly update," Proceedings of SPIE: Imaging Spectrometry XVIII (8870) (2013).

[7] Lucke, R. L., Corson, M., McGlothlin, N. R., Butcher, S. D., Wood, D. L., Korwan, D. R., Li, R. R., Snyder, W. A., Davis, C. O., and Chen, D. T., "Hyperspectral imager for the coastal ocean: instrument description and first images," *Appl. Opt.* **50**, 1501–1516 (Apr 2011).

[8] Gege, P., "Analytic model for the direct and diffuse components of downwelling spectral irradiance in water," *Appl. Opt.* **51**, 1407–1419 (Mar 2012).

[9] Kotchenova, S. Y., Vermote, E. F., Matarrese, R., and Frank J. Klemm, J., "Validation of a vector version of the 6s radiative transfer code for atmospheric correction of satellite data. part i: Path radiance," *Appl. Opt.* **45**, 6762–6774 (Sep 2006).